# *Strengthening mechanism of additively manufactured cold spray Al deposits under low deposition efficiency*

***Ningsong Fan, Richard Jenkins, Pengfei Yu, Rocco Lupoi, Shuo Yin***
*Trinity College Dublin, The University of Dublin, Department of Mechanical, Manufacturing & Biomedical Engineering, Parsons Building, Dublin 2, Ireland*

***Jan Cizek***
*Institute of Plasma Physics, The Czech Academy of Sciences, Za Slovankou 1782/3, 182 00, Prague, Czech Republic*
*Institute of Materials Science and Engineering, Brno University of Technology, Technicka 2896/2, 616 69, Brno, Czech Republic*

## Abstract

In this study, a novel strategy to manufacture high strength cold-sprayed Al coating by using powder with wide size distribution is proposed. The microstructure and mechanical properties of deposited coating sprayed at three typical impact velocities before and after heat treatment are investigated. Furthermore, the deposition and strengthening mechanisms of the coating sprayed at various impact velocities are clarified. The results show that the coating with higher density and mechanical properties can be successfully fabricated by cold spray at comparatively low particle impact velocity. The mechanical properties were enhanced with the contribution of heat treatment process. It is the in-process tamping effect induced by larger powder that results in the severe plastic deformation thus leads to densification and excellent mechanical properties of the cold-sprayed Al coating.

**Keywords**
Cold spray, Coating, Microstructure, Mechanical Prosperities.

## Introduction

Cold spray additive manufacturing (CSAM) is a rapid solid-state deposition process which can be utilized to manufacture freestanding parts, fabricate coating on the substrate and repair damaged components (Ref 1,2). This additive manufacturing technique has been applied for deposition of various metallic materials with certain plasticity including pure metals, alloys, high entropy alloys as well as amorphous alloys (Ref 3–5). Fig.1 shows a schematic of cold spray additive manufacturing technology. In the process of cold spray, metal feedstock particles are accelerated by compressed gas (typically nitrogen, helium, or the mixture of the two (Ref 6)) and then impact onto a target substrate with high kinetic energy. The particles experience severe plastic deformation to form a coating with effective bonding at temperatures below their melting point which makes it extremely different and special to other fusion-based additive manufacturing methods. Impact velocity is the key of particles deposition and attachment as the particles will rebound from the substrate if they fail to reach or exceed a certain value of critical velocity. The value of critical velocity is dependent on many factors such as the types of substrate and feedstock powder, particle size and geometry, and cold spray processing parameters (Ref 7–9). Various particle impact velocities can be reached by selecting the different combination of gas type, process gas pressure and temperature. It is generally accepted that higher quality coating will be produced with the increment of impact velocity as more severe plastic deformation undergone on the deposited particle. Several researches have been conducted by performing experiments. The investigation performed by Wang et al. found that the hardness and bond strength of purity Al coating fabricated by CSAM were enhanced with the increase of impact velocity from 610 to 710 m/s (Ref 10). Meng et al. investigated the effect of gas temperature on the microstructure and mechanical properties of cold-sprayed 304 stainless steel coating and the results showed that both the relative density and cohesive strength of the coating increased when the gas temperature rose from 450 to 550 °C (Ref 11). The work of Huang et al. showed that the tensile strength of Cu coating increased with the growth of particle velocity which was achieved by changing gas from nitrogen to expensive helium and increasing the gas temperature and pressure (Ref 12). Sudharshan Phani et al. reported the influence of particle velocity on porosity and microhardness of the copper coating which revealed that lower porosity and higher microhardness were achieved with the increasing particle velocity (Ref 13). The literatures mentioned above came to a unanimous conclusion: both the densification and mechanical properties were improved or enhanced with the increment of particle impact velocity. However, in our previous work investigating cold-sprayed Al coating (Ref 14), it has been found that with the growing of feedstock impact velocity, the particle plastic deformation rate and coating density decreased initially and then followed an increment which is contrary to common views. In other words, low particle impact velocity can lead to a coating with low porosity.

Mechanical properties have been widely concerned which significantly decide the properties and performance of coating fabricated by cold spray additive manufacturing. However, previous investigation showed that the mechanical properties of as-sprayed coating were poor during the cold spray process due to the existence of residual stress and work hardening effect (Ref 15). The general way to further enhanced the mechanical

properties of the CS deposits is via post heat treatment which was reported in some literatures (Ref 15–18). In this study, a further investigation was performed to study the microstructure and mechanical properties of Al coating sprayed at relatively low impact velocity. In addition, the effect of heat treatment on microstructure and mechanical properties of the coating was also discussed.

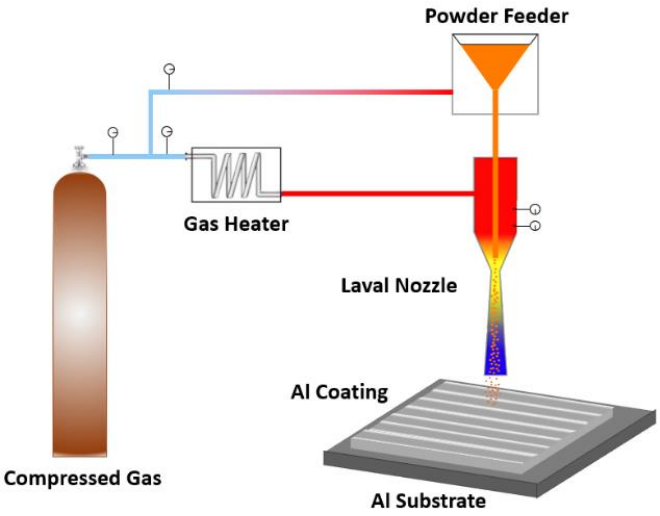


*Fig.1. Schematic of cold spray additive manufacturing technology*

## Experimental methodology

### Coating fabrication procedure

Spherical Al powders (H-30, Valimet Inc., California) were used as the cold spraying feedstock and the nominal chemical components of the feedstock were listed in Table 1. The powder diameter ranges from 4 to 62 μm with a mean size of 40 μm. The surface morphology was observed by scanning electron microscope (SEM, Carl Zeiss ULTRA Plus, Germany) as Fig. 2 showed. The coating was manufactured with an in-house cold spray system (Trinity College Dublin, Ireland) on the thin aluminium substrate. The cold spray equipment is mainly composed of high temperature gas supply, gas heater, powder feeder, CNC platform, de-Laval nozzle and computer control and monitoring system (Ref 19) . Based on the results of previous study, the density of Al coating firstly decreased with the temperature rising from 300 to 650℃ using nitrogen at 3.0Mpa, then increased with the pressure rising from 1.5 to 3.0Mpa in an atmosphere of helium at 20℃ . Hence, as Table 2 showed, three typical working parameters were selected to obtain different particle impact velocities and studied the variation trend of coating strength with impact velocities which were calculated at 640, 770 and 1000m/s respectively by the computational fluid dynamic (CFD) model mentioned in our previous work (Ref 20). Furthermore, post heat treatment was performed by tube furnace (Clare 4.0, Clasic, Czech Republic) for half of the samples with the purpose of improving coating mechanical properties. The heat treatment process was carried out at heating ramp rate of 6 ℃/min to the temperature of 300℃ for 4h in the argon-7.5% hydrogen atmosphere and the specimens were then furnace cooled to room temperature.

*Table 1. Nominal chemical components of Al powders*

| Components | Aluminum | Iron | Oil & Grease | Volatile |
|---|---|---|---|---|
| Wt.% | > 99.7 | < 0.2 | < 0.2 | < 0.1 |

### Materials characterization

Microstructural analysis was performed including samples mounting, metallographic abrasive grinding with P180, P1200, P2500 SiC paper and polishing to a mirror finish with 6, 1 and 0.06 μm silica suspension respectively. The samples were then etched with Keller's Reagent (PD1608-095-250, UK) to better reveal their phase microstructure and the cross-sectional morphology of sprayed coating was characterized by SEM. Moreover, the total porosity of the coating from cross-section micrographs was estimated by the optical microscope (OM, Leica DM LM, Germany) and then calculated by the image analysis software (ImageJ, National Institutes of Health, USA). The original cross-sectional images were represented in the binary mode and the area ratio of black pores were defined as coating porosity. Five measurements were performed to ensure the data reliability, and the average value was considered as the final porosity.

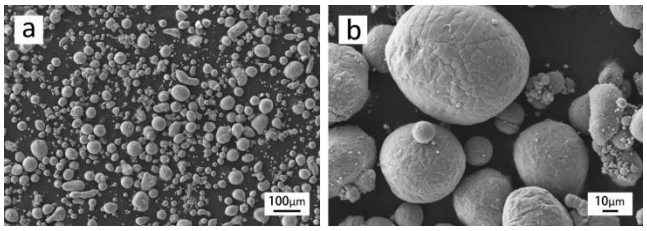


*Fig.2. Surface morphology of the Al feedstock used in the coating fabrication.*
*Low magnification (b) High magnification*

*Table 2. Experimental parameters of cold spray process used in this work.*

| Experiment No. | Sample 1 | Sample 2 | Sample 3 |
|---|---|---|---|
| Pressure /MPa | 3.0 | 3.0 | 3.0 |
| Temperature /°C | 300 | 650 | 20 |
| Nozzle Traverse speed / mm/s | 50 | 50 | 50 |
| Standoff distance /mm | 30 | 30 | 30 |
| Propulsive gas | $N_2$ | $N_2$ | He |
| Particle impact velocity/ m/s | 640 | 770 | 1000 |

### Mechanical Properties

Microhardness reflects the basic mechanical properties and the density of cold- sprayed coating. Therefore, the microhardness of fabricated coating was measured by Vickers hardness indenter (MVK-H1, Mitutoyo, Japan) with an applied load of 100g for 10s at room temperature. For each of the sample, 12 indentations were carried out on the cross-section of the polished Al coating randomly. The highest and lowest value were abandoned, and the average value computed as the result

of the microhardness. The typical morphology of indentation was characterized by OM. In order to determine the mechanical properties of the cold-sprayed aluminum coating, the sample was machined into a dog-bone shape and evaluated on the tensile testing machine (Instron 3366, US) at a displacement rate of 1 mm/min till a complete fracture of the sample. The ultimate tensile strength (UTS) and elongation at break (EL) were dependent on the average value of three specimens. The typical fracture morphology of the specimens was then observed using SEM to analyse and understand the failure mechanism.

## Results and discussion

**Coating Microstructure**

Fig.3 shows the cross-sectional images of Al coating in the as-sprayed state and after heat treatment with different particle impact velocities. As shown in Fig.3(a)-(c), the coating fabricated at the impact velocity of 640 and 1000m/s exhibit quite dense structure while coating sprayed at 770m/s appears pores and cracks. That is to say, the particles impacting onto the substrate with higher kinetic energy do not always lead to a denser coating. The calculated results of porosity before and after annealing were shown in Fig.4 where the observation was further proved. It can be found that the porosity of coating sprayed at 640m/s is 0.07% which is much lower than that of the other two coatings: 4.24 and 1.53% respectively. The high porosity of the coating sprayed at 770m/s is due to the insufficient deformation of particles around the pores and cracks in the deposition process. After heat treatment, the coatings were denser, and the size of pores also became smaller compared with the as-sprayed ones as shown in Fig.3(d)-(f). The porosity was slightly decreased especially for the coating sprayed at the impact velocity of 770 and 1000 m/s and the range of error bars were also reduced. During the heat treatment process, some of the interface line between particles were healed with the contribution of diffusion effect. However, there is no obvious change in porosity of coating sprayed at the impact velocity of 640 m/s after annealing.

Fig. 4 shows a graph with the recorded level of impact velocity versus coating porosity. The deposition efficiency measured (DE) was 1.66% for the lower velocity case, 17.45% for the medium velocity case, 64.99% higher velocity case. Fig.5 shows the etched cross-sectional images and binary images of as-sprayed Al coating with different particle impact velocities. Based on the boundaries revealed in the images, it can be observed that the spherical Al powders were flattened in different levels after deposition. The deposited particles sprayed at 300℃using nitrogen undergone much more significant plastic deformation where the spherical powders squashed into long strips typically in the deposition direction and the particles interlocked tightly with each other. This is in stark contrast to the coating fabricated at 650℃: even though the higher particle impact velocity was obtained by increasing temperature, the flattening level of the particles were much less and pores between particles are clearly visible which means the particles experienced less plastic deformation. As the impact velocity continues to increase by using helium, the particles deformed more severely and the pores came to be smaller and even disappeared. So, it can be inferred that it is the serious plastic deformation experienced by the particles that lead to a dense coating.

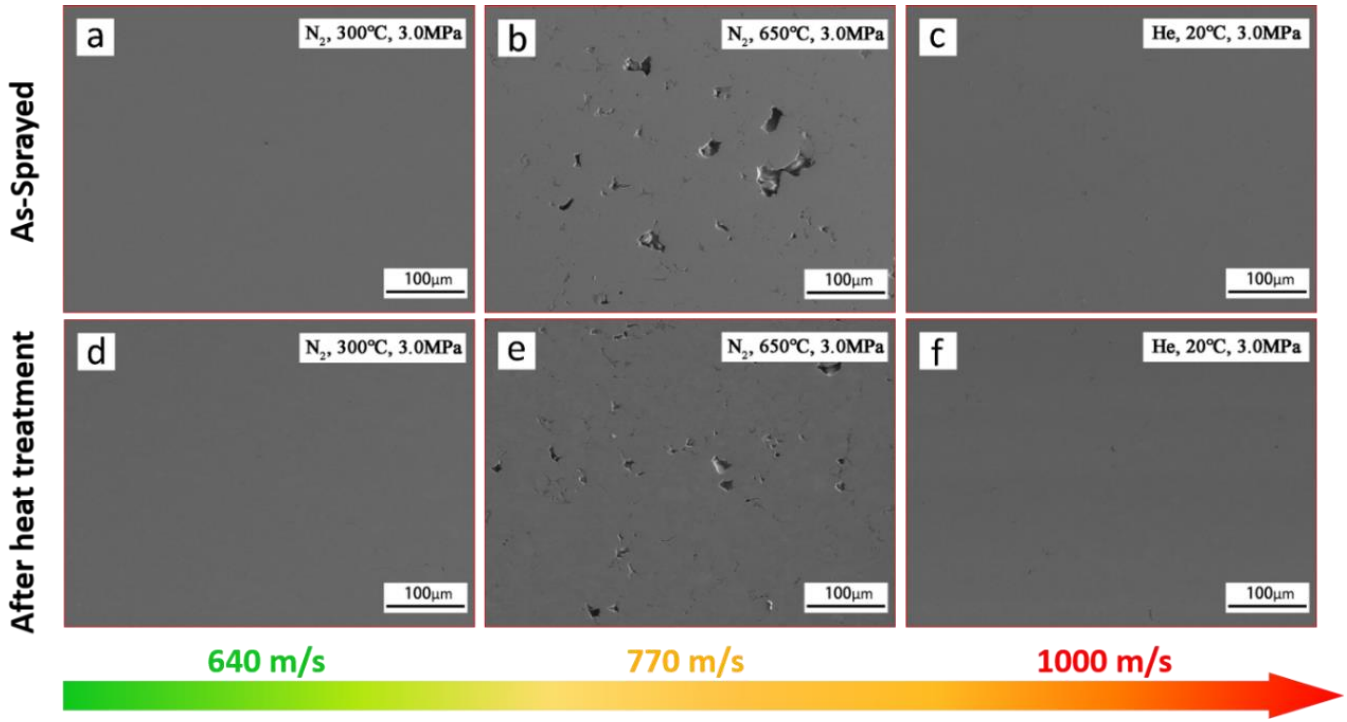


*Fig.3. Cross-sectional images of Al coating in the as-sprayed state (upper row) and after heat treatment (lower row) with different particle impact velocities. (a) (d)640m/s, (b)(e)770m/s, (c)(f)1000m/s*

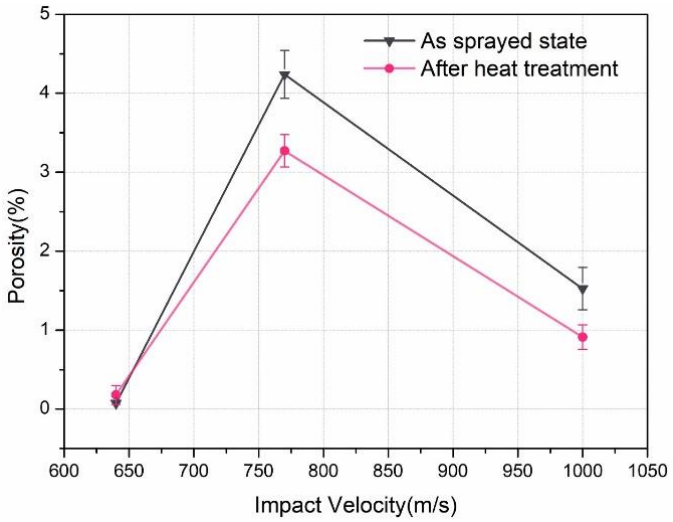


*Fig.4. Porosity of the cold-sprayed Al coating before and after annealing*

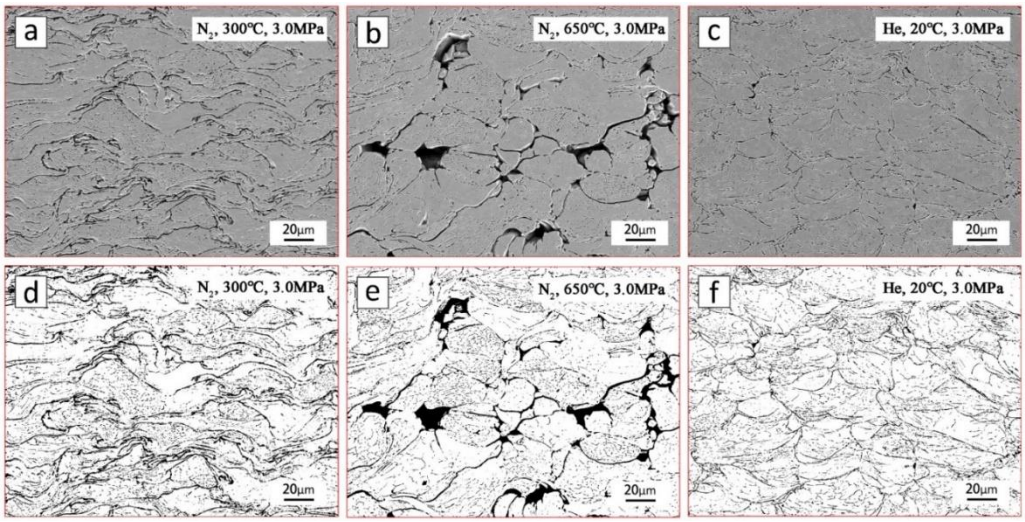


*Fig.5. Etched Cross-sectional images (upper row) and binary images (lower row) of as-sprayed Al coating with different particle impact velocities. (a) (d)640m/s, (b)(e)770m/s, (c)(f)1000m/s*

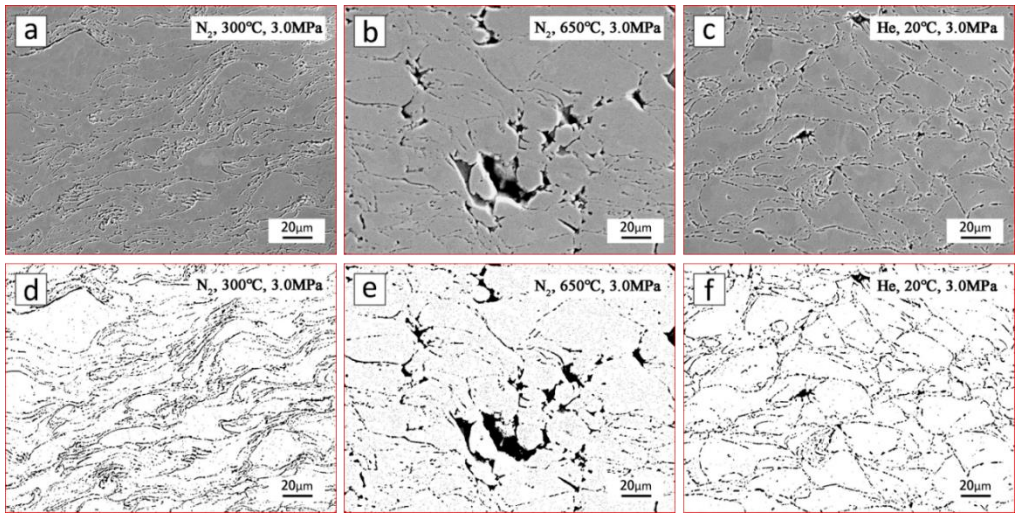


*Fig.6. Etched cross-sectional images (upper row) and binary images (lower row) of Al coating after heat treatment with different particle impact velocities. (a) (d)640m/s, (b)(e)770m/s, (c)(f)1000m/s*

Fig.6 shows the etched cross-sectional images and binary images of Al coating after heat treatment with different particle impact velocities. It seems that some particle-to-particle interfaces were less visible after annealing. However, the general microstructure with the action of heat treatment changed inconspicuously when compared with the as-sprayed one.

**Microhardness and tensile strength**

Fig.7 shows the microhardness of the cold-sprayed Al coating and morphology of indentations in the as-sprayed state and after heat treatment. It is evident that the Al coating produced at the particle impact velocity of 640m/s exhibits approximate microhardness to that of the coating sprayed at 1000 m/s, which is higher than the coating sprayed at 770 m/s. This observation is due to the quite different porosity level of the coating. Furthermore, there are some microcracks around the indentations among the three coatings in the as-sprayed state. The microhardness of the coating fell after post-annealing due to the removal of work hardening. The indentations kept good diamond shape and no obvious micro-cracks showed near the indentations.

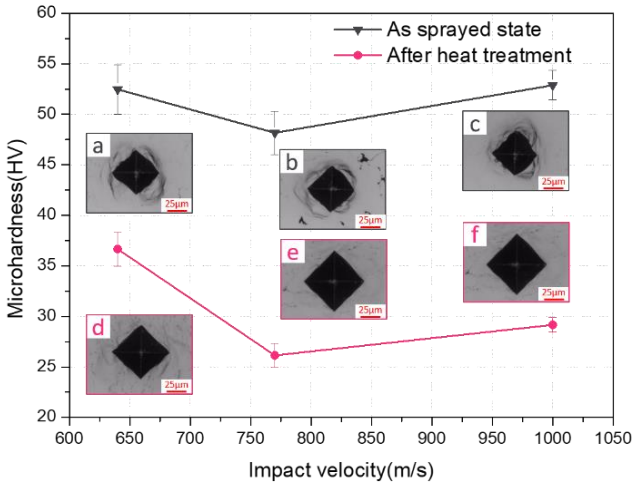


*Fig.7. Microhardness of the cold-sprayed Al coating and morphology of indentation in the as-sprayed state and after heat treatment*

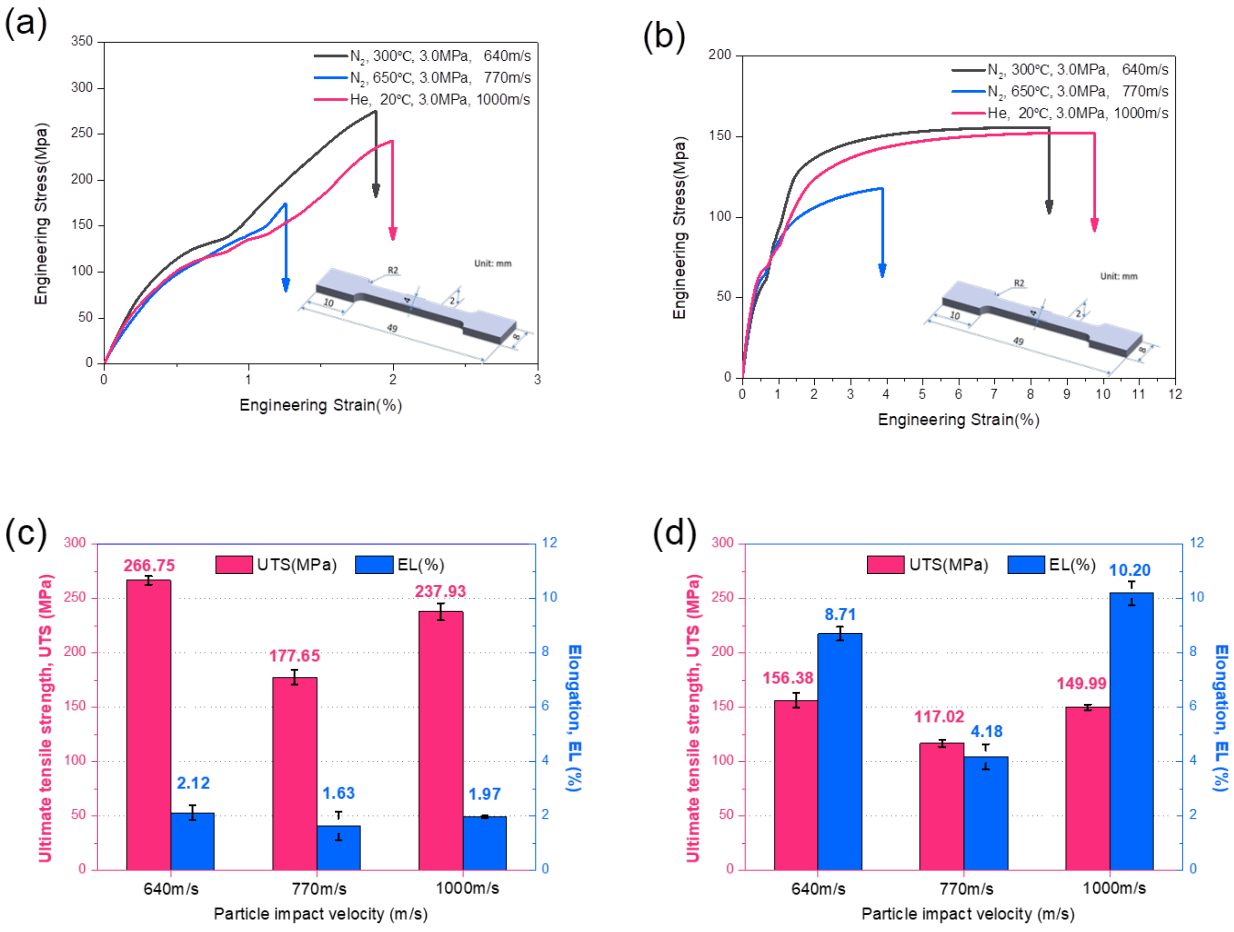


*Fig.8. The representative stress-strain curves, ultimate tensile strength (UTS) and elongation (EL) of cold-sprayed Al coating with different particle velocities. (a)(c) as-sprayed; (b)(d) after annealing*

Fig.8 shows the representative stress-strain curves, ultimate tensile strength (UTS) and elongation (EL) of cold-sprayed Al coating with different particle velocities before and after annealing. As can be seen from Fig.8 (a) and (c), all the as-sprayed Al coatings have poor ductility. The coating sprayed at the impact velocity of 770 m/s had lower ultimate tensile strength and elongation compared with the ones at 640 and 1000 m/s owing to the porous structure and poor inter-particle bonding. After heat treatment, the ductility of all the coatings significantly improved and the Al coatings sprayed at the impact velocity of 640, 770, 1000m/s possessed EL of about 8.71, 4.18, 10.20% respectively as shown in Fig.8 (b) and (d). The UTS decreased sharply because of the removal of work hardening effect after heat treatment particularly for the coating sprayed at the impact velocity of 640 m/s which experienced more severe plastic deformation in the deposition stage.

Fig.9 shows the fractographic images of the cold-sprayed Al coating in the as-deposited state. As shown in Fig.9 (a) and (b), the layer-by-layer structure in the direction of deposition is clearly discernible and the fracture occurred from the interfaces between deposited particles. Limited dimple can be seen on the interface of the particles which corresponds the failure mode was brittle fracture. For the coating with the lowest UTS and EL which was sprayed at the impact velocity of 770 m/s, the interfacial bonding between particles was weak and the surface of fracture particle was smooth as Fig.9 (c) and (d) showed. The fractographic images showed in Fig.9 (e) and (f) are different from the aforementioned ones. It seems that metallurgical bonding took place between particles.

Fig.10 shows the fractographic images of the cold-sprayed Al coating after heat treatment. A number of dimples were formed at the tensile fracture which was an obvious sign of ductile fracture. As shown in Fig.10 (e) and (f), the dimples were both deep and large which illustrated that the resistance of crack propagation was comparatively large. The ductility was greatly improved with the contribution of annealing process where the EL increased from 1.97 to 10.20%.

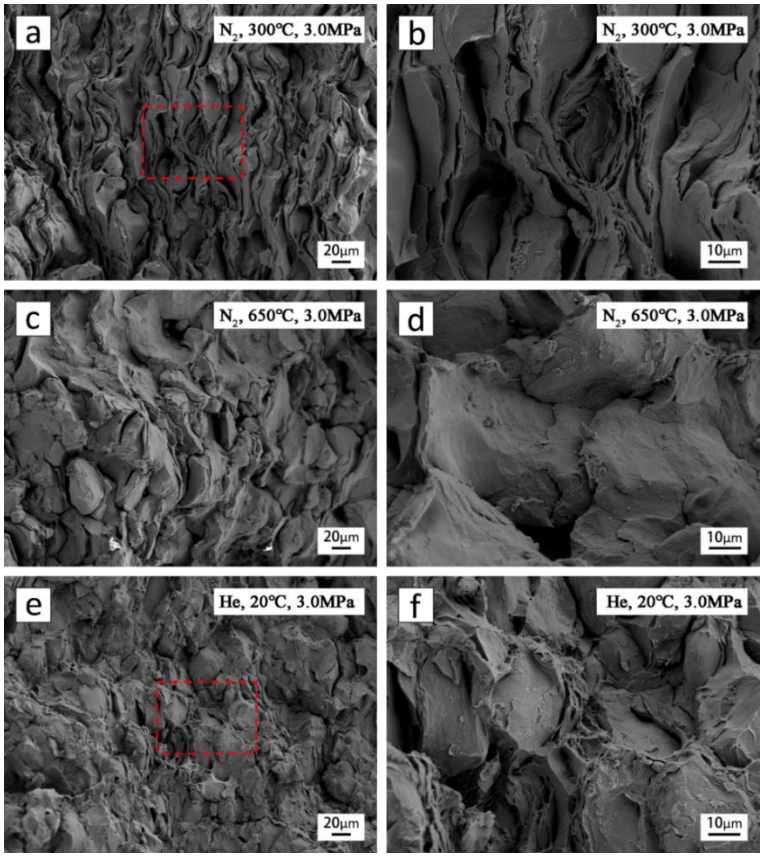


*Fig 9. Fractographic images of the cold-sprayed Al coating in the as-depoisted state. (a) (b)640m/s, (c)(d)770m/s, (e)(f)1000m/s*

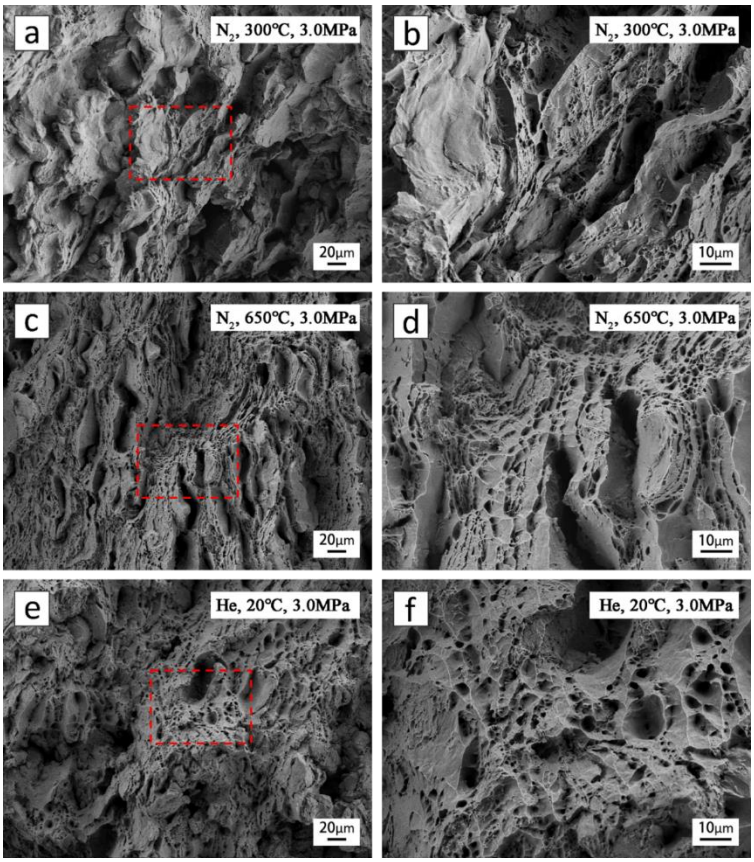


*Fig.10. Fractographic images of the cold-sprayed Al coating after heat treatment (a) (b)640m/s, (c)(d)770m/s, (e)(f)1000m/s*

**Deposition mechanism**

Fig.11 shows the schematic of deposition mechanism for Al coating sprayed at the impact velocity of 640, 770 and 1000 m/s respectively. The feedstock used in this experiment possess a wide powder size distribution and this is also represented in the picture with various sizes of grey balls. As shown in Fig.11 (a), some of the smaller Al powder successfully deposited to form coating at 300℃ in the atmosphere of nitrogen. However, for the powders with larger size, they rebounded from the substrate after impacting because of the insufficient kinetic energy. In this process, the undeposited particles hit the coating and made the deposits experienced more plastic deformation. The deposits were flattened to thin and long strips by multiple tamping and hammer, thus interlocked with each other. There are few pores and cracks in the cold spray coating and the mechanical strength is significantly excellent which can be attributed to the tamping effect. When the temperature rose to 650℃, some of the larger powder obtained enough kinetic energy and started to deposit as the critical velocity decreased with the growing of temperature. The number of powders that enable to tamp and hammer the coating was dramatically reduced. The degree of plastic deformation of the particles declined which leads to pores shown in Fig.11 (b). The porous structure resulted in low microhardness and coating strength. Fig.11 (c) illustrates the situation using helium where the particle impact velocity increased to 1000 m/s. The higher velocities enabled most of the powders including larger ones to deposit and deeply embedded. The primary difference from the particles sprayed at 770 m/s is that the particles sprayed at 1000 m/s undergone more severe plastic deformation which resulted in stronger work hardening effect and thus conduced to better mechanical properties as the one sprayed at 640 m/s. Based on the above analysis, it can be concluded that the in-process tamping effect plays a vital role in the coating densification and high coating strength.

Although the coating with lower porosity and more excellent mechanical properties may be fabricated by increasing temperature (>650℃) in the atmosphere of nitrogen, some technical problems will be followed. It is reported that the increased gas temperature will lead to oxidation, nitridation and damage of the sensitivity cold spray nozzle (Ref 21). Moreover, excessive impact velocity will bring about corrosion on the substrate surface (Ref 22,23). The problems above can be avoided with the usage of helium. However, the high cost of helium is obvious economically unfavourable. The work conducted by previous researchers show that the coating density and mechanical properties were enhanced with the effect of tamping and hammering by introducing large size particles, such as mixing large stainless steel particles into the IN718, Ti6Al4V and Ti powder (Ref 24,25), adding $Al_2O_3$ particles to A380 alloy powder (Ref 26) and mingling $Cu_2O$ particles to Cu powders (Ref 27). Nevertheless, the second

phase particles are likely to stimulate stress concentrations and generate pores. By comparison, the novel strategy for manufacturing good quality cold-sprayed coating by using feedstock with wide range distribution is more advantageous and economical. Ti6Al4V and Ti powder (Ref 24,25), adding $Al_2O_3$ particles to A380 alloy powder (Ref 26) and mingling $Cu_2O$ particles to Cu powders (Ref 27). Nevertheless, the second phase particles are likely to stimulate stress concentrations and generate pores. The problems above can be avoided with the usage of helium. However, the high cost of helium is obvious economically unfavourable. By comparison, the novel strategy for manufacturing good quality cold-sprayed coating by using feedstock with wide range distribution can be more advantageous and economical.

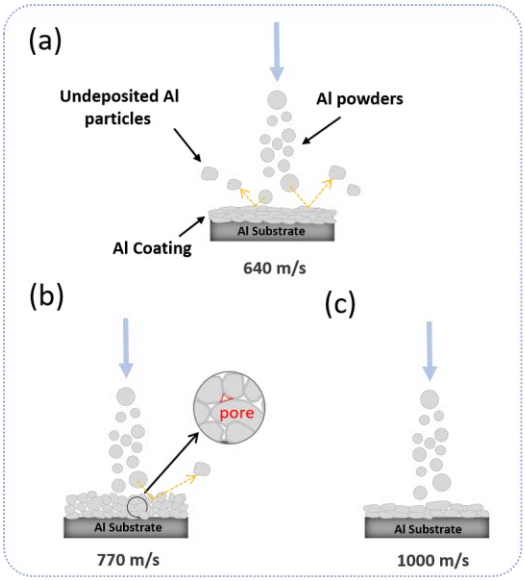


*Fig.11. Schematic of deposition mechanism for Al coating sprayed at the impact velocity of (a)640 m/s (b)770 m/s and (c) 1000 m/s*

## Conclusions

In this study, the microstructure of Al coating manufactured by cold spray at three typical impact velocities were characterized. The porosity, microhardness and tensile test were performed to evaluate coating mechanical properties. Furthermore, the effect of heat treatment on the improvement of microstructure and mechanical properties was also discussed. Based on the experiment results, the following conclusions can be drawn:

1. The cold-sprayed Al coating fabricated at the impact velocity of 640 m/s possessed extremely lower porosity, higher microhardness, UTS and EL than that of coating sprayed at 770 and 1000 m/s both in the as-sprayed state and after heat treatment.

2. Post heat treatment optimize the microstructure and enhance the resultant mechanical properties of cold-sprayed Al coating.

3. In-process tamping effect induced by larger powder results in the severe plastic deformation thus leads to densification and excellent mechanical properties of the cold-sprayed Al coating. The usage of powder with wide size distribution conduce to fabricate density as well as high strength coating by CS.

## Acknowledgements

The first author of this work is supported by the China Scholarship Council (No.201906460020). The authors also acknowledge the CRANN Advanced Microscopy Laboratory (AML) of Trinity College Dublin for the support in data analysis.

## REFERENCES

1. W. Li, K. Yang, S. Yin, X. Yang, Y. Xu, and R. Lupoi, Solid-State Additive Manufacturing and Repairing by Cold Spraying: A Review, *J. Mater. Sci. Technol.*, Elsevier, 2018, **34**(3), p 440–457.
2. S. Yin, P. Cavaliere, B. Aldwell, R. Jenkins, H.L. Liao, W.Y. Li, and R. Lupoi, Cold Spray Additive Manufacturing and Repair: Fundamentals and Applications, *Addit. Manuf.*, 2018, **21**, p 628–650.
3. R.N. Raoelison, Y. Xie, T. Sapanathan, M.P. Planche, R. Kromer, S. Costil, and C. Langlade, Cold Gas Dynamic Spray Technology: A Comprehensive Review of Processing Conditions for Various Technological Developments till to Date, *Addit. Manuf.*, Elsevier, 2018, **19**, p 134–159.
4. S. Yin, W. Li, B. Song, X. Yan, M. Kuang, Y. Xu, K. Wen, and R. Lupoi, Deposition of FeCoNiCrMn High Entropy Alloy (HEA) Coating via Cold Spraying, *J. Mater. Sci. Technol.*, Elsevier, 2019, **35**(6), p 1003–1007.
5. A. Moridi, S.M. Hassani-Gangaraj, M. Guagliano, and M. Dao, Cold Spray Coating: Review of Material Systems and Future Perspectives, *Surf. Eng.*, Taylor & Francis, 2014, **30**(6), p 369–395.
6. W. Wong, E. Irissou, A.N. Ryabinin, J.-G. Legoux, and S. Yue, Influence of Helium and Nitrogen Gases on the Properties of Cold Gas Dynamic Sprayed Pure Titanium Coatings, *J. Therm. Spray Technol.*, Springer, 2011, **20**(1–2), p 213–226.
7. F. Raletz, M. Vardelle, and G. Ezo'o, Critical Particle Velocity under Cold Spray Conditions, *Surf. Coatings Technol.*, Elsevier, 2006, **201**(5), p 1942–1947.
8. C.-J. Li, W.-Y. Li, and H. Liao, Examination of the Critical Velocity for Deposition of Particles in Cold Spraying, *J. Therm. Spray Technol.*, Springer, 2006, **15**(2), p 212–222.
9. H. Assadi, F. Gärtner, T. Stoltenhoff, and H. Kreye, Bonding Mechanism in Cold Gas Spraying, *Acta Mater.*, 2003, **51**(15), p 4379–4394, doi:https://doi.org/10.1016/S1359-6454(03)00274-X.

10. Q. Wang, N. Birbilis, and M.-X. Zhang, Process Optimisation of Cold Spray Al Coating on AZ91 Alloy, *Surf. Eng.*, Taylor & Francis, 2014, **30**(5), p 323–328.
11. X. Meng, J. Zhang, J. Zhao, Y. Liang, and Y. Zhang, Influence of Gas Temperature on Microstructure and Properties of Cold Spray 304SS Coating, *J. Mater. Sci. Technol.*, 2011, **27**(9), p 809–815, doi:https://doi.org/10.1016/S1005-0302(11)60147-3.
12. R. Huang and H. Fukanuma, Study of the Influence of Particle Velocity on Adhesive Strength of Cold Spray Deposits, *J. Therm. spray Technol.*, Springer, 2012, **21**(3–4), p 541–549.
13. P.S. Phani, D.S. Rao, S. V Joshi, and G. Sundararajan, Effect of Process Parameters and Heat Treatments on Properties of Cold Sprayed Copper Coatings, *J. Therm. Spray Technol.*, Springer, 2007, **16**(3), p 425–434.
14. R. Jenkins, S. Yin, B. Aldwell, M. Meyer, and R. Lupoi, New Insights into the In-Process Densification Mechanism of Cold Spray Al Coatings: Low Deposition Efficiency Induced Densification, *J. Mater. Sci. Technol.*, The editorial office of Journal of Materials Science & Technology, 2019, **35**(3), p 427–431.
15. R. Huang, M. Sone, W. Ma, and H. Fukanuma, The Effects of Heat Treatment on the Mechanical Properties of Cold-Sprayed Coatings, *Surf. Coatings Technol.*, Elsevier, 2015, **261**, p 278–288.
16. P.S. Phani, V. Vishnukanthan, and G. Sundararajan, Effect of Heat Treatment on Properties of Cold Sprayed Nanocrystalline Copper Alumina Coatings, *Acta Mater.*, Elsevier, 2007, **55**(14), p 4741–4751.
17. M. Yu, W.-Y. Li, C. Zhang, and H. Liao, Effect of Vacuum Heat Treatment on Tensile Strength and Fracture Performance of Cold-Sprayed Cu-4Cr-2Nb Coatings, *Appl. Surf. Sci.*, Elsevier, 2011, **257**(14), p 5972–5976.
18. X. Qiu, J. Wang, L. Gyansah, J. Zhang, and T. Xiong, Effect of Heat Treatment on Microstructure and Mechanical Properties of A380 Aluminum Alloy Deposited by Cold Spray, *J. Therm. Spray Technol.*, Springer, 2017, **26**(8), p 1898–1907.
19. S. Yin, R. Jenkins, X. Yan, and R. Lupoi, Microstructure and Mechanical Anisotropy of Additively Manufactured Cold Spray Copper Deposits, *Mater. Sci. Eng. A*, Elsevier B.V., 2018, **734**(January), p 67–76.
20. S. Yin, Y. Xie, X. Suo, H. Liao, and X. Wang, "Interfacial Bonding Features of Ni Coating on Al Substrate with Different Surface Pretreatments in Cold Spray," *Materials Letters*, 2015, p 143–147.
21. V.K. Champagne, "The Cold Spray Materials Deposition Process," *The cold spray materials deposition process*, 2007.
22. T. Schmidt, F. Gärtner, H. Assadi, and H. Kreye, Development of a Generalized Parameter Window for Cold Spray Deposition, *Acta Mater.*, 2006, **54**(3), p 729–742.
23. T. Schmidt, F. Gaertner, and H. Kreye, New Developments in Cold Spray Based on Higher Gas and Particle Temperatures, *J. Therm. Spray Technol.*, Springer, 2006, **15**(4), p 488–494.
24. X.-T. Luo, Y.-K. Wei, Y. Wang, and C.-J. Li, Microstructure and Mechanical Property of Ti and Ti6Al4V Prepared by an In-Situ Shot Peening Assisted Cold Spraying, *Mater. Des.*, Elsevier, 2015, **85**, p 527–533.
25. X.T. Luo, M.L. Yao, N. Ma, M. Takahashi, and C.J. Li, Deposition Behavior, Microstructure and Mechanical Properties of an in-Situ Micro-Forging Assisted Cold Spray Enabled Additively Manufactured Inconel 718 Alloy, *Mater. Des.*, Elsevier Ltd, 2018, **155**, p 384–395.
26. X. Qiu, N. ul H. Tariq, L. Qi, J.Q. Wang, and T.Y. Xiong, A Hybrid Approach to Improve Microstructure and Mechanical Properties of Cold Spray Additively Manufactured A380 Aluminum Composites, *Mater. Sci. Eng. A*, 2020, **772**(September 2019).
27. D. Rui, X. Li, W. Jia, W. Li, W. Xiao, and T. Gui, Releasing Kinetics of Dissolved Copper and Antifouling Mechanism of Cold Sprayed Copper Composite Coatings for Submarine Screen Doors of Ships, *J. Alloys Compd.*, Elsevier B.V, 2018, **763**, p 525–537.